



## Estimating global cropland production from 1961 to 2010

Pengfei Han<sup>1\*</sup>, Ning Zeng<sup>1,2\*</sup>, Fang Zhao<sup>2,3</sup>, Xiaohui Lin<sup>4</sup>

<sup>1</sup>State Key Laboratory of Numerical Modeling for Atmospheric Sciences and Geophysical Fluid Dynamics, Institute of Atmospheric Physics, Chinese Academy of Sciences, Beijing 100029, China

<sup>2</sup>Department of Atmospheric and Oceanic Science, and Earth System Science Interdisciplinary Center, University of Maryland, College Park, Maryland 20742, USA

<sup>3</sup>Potsdam Institute for Climate Impact Research, Potsdam, Brandenburg 14473, Germany

<sup>4</sup>State Key Laboratory of Atmospheric Boundary Layer Physics and Atmospheric Chemistry, Institute of Atmospheric Physics, Chinese Academy of Sciences, Beijing 100029, China

*Correspondence to:*

Ning Zeng (zeng@lasg.iap.ac.cn);

Pengfei Han (pfhan@mail.iap.ac.cn)



1 **Abstract.** Global cropland net primary production (NPP) has tripled over the last fifty  
2 years, contributing 17-45 % to the increase of global atmospheric CO<sub>2</sub> seasonal  
3 amplitude. Although many regional-scale comparisons have been made between  
4 statistical data and modelling results, long-term national comparisons across global  
5 croplands are scarce due to the lack of detailed spatial-temporal management data.  
6 Here, we conducted a simulation study of global cropland NPP from 1961 to 2010  
7 using a process-based model called VEGAS and compared the results with Food and  
8 Agriculture Organization of the United Nations (FAO) statistical data on both  
9 continental and country scales. According to the FAO data, the global cropland NPP  
10 was 1.3, 1.8, 2.2, 2.6, 3.0 and 3.6 PgC yr<sup>-1</sup> in the 1960s, 1970s, 1980s, 1990s, 2000s  
11 and 2010s, respectively. The VEGAS model captured these major trends at global and  
12 continental scales. The NPP increased most notably in the U.S. Midwest, Western  
13 Europe and the North China Plain, and increased modestly in Africa and Oceania.  
14 However, significant biases remained in some regions such as Africa and Oceania,  
15 especially in temporal evolution. This finding is not surprising as VEGAS is the first  
16 global carbon cycle model with full parameterization representing the Green  
17 Revolution. To improve model performance for different major regions, we modified  
18 the default values of management intensity associated with the agricultural Green  
19 Revolution differences across various regions to better match the FAO statistical data  
20 at the continental level and for selected countries. Across all the selected countries,  
21 the updated results reduced the root mean square error (RMSE) from 19.0 to 10.5 TgC  
22 yr<sup>-1</sup> (~45 % decrease). The results suggest that these regional differences in model  
23 parameterization are due to differences in social-economic development. To better  
24 explain the past changes and predict the future trends, it is important to calibrate key  
25 parameters at regional scales and develop datasets for land management history.



## 26 **1 Introduction**

27 Cropland net primary production (NPP) plays a crucial role in both food security  
28 and atmospheric CO<sub>2</sub> variations. Crop yield is part of crop NPP, thus food security  
29 relies greatly on crop NPP. It has been reported that increase in cropland NPP driven  
30 by the agricultural Green Revolution contributed 17-45 % of the increase in  
31 atmospheric CO<sub>2</sub> seasonal amplitude (Gray et al., 2014; Zeng et al., 2014).  
32 Furthermore, vegetation is the most active C reservoir in the terrestrial ecosystem, and  
33 is easily affected by climate change (e.g., drought) and management practices, thus  
34 potentially affecting global climate change (Le Quéré et al., 2016; Zeng et al., 2005b;  
35 Zhao and Running, 2010).

36 Globally, agricultural areas cover ~1,370 million hectares (Mha), distributed across  
37 diverse climatic and edaphic conditions, with a variety of complex cropping systems  
38 and management practices (Foley et al., 2011; Gray et al., 2014; Lal, 2004; Monfreda  
39 et al., 2008). Features of the agricultural Green Revolution include 1) adoption of  
40 improved varieties, 2) expansion of irrigation, and 3) increased use of chemical  
41 fertilizer and pesticide. These three factors have contributed approximately equally to  
42 increased crop NPP (Sinclair, 1998). Although the agricultural Green Revolution has  
43 been identified as a key driver of increased crop yield, its impact on crop NPP differs  
44 across time and space. Management intensity (here, mainly referring to the third  
45 feature of the Green Revolution) varies largely and has not always changed  
46 synchronously in different parts of the world (Table 1) (Ejeta, 2010; Evenson, 2005;  
47 Glaeser, 2010; Hazell, 2009). Thus, cropland NPP is highly variable, complicating the  
48 assessment of global cropland NPP (Bondeau et al., 2007; Ciais et al., 2007; Gray et  
49 al., 2014). For example, in the USA, the timing and magnitude of the agricultural  
50 Green Revolution occurred almost evenly from 1961-2010, while in Brazil, the most  
51 dramatic increase occurred after 2000 (Glaeser, 2010; Hazell, 2009). However,  
52 accounting for such effects of heterogeneity in management practices over time and  
53 space on crop NPP at a global scale has been rare to date.



54 Three methods are available for estimating vegetation NPP: statistical data,  
55 process-based models and remote sensing. Statistical data and process-based models  
56 are prevalent method for estimating global NPP, but, except for a few recent studies,  
57 are generally limited to natural vegetation based on climate and edaphic variables,  
58 (Gray et al., 2014; Zeng et al., 2014). Therefore, global- and regional-scale estimates  
59 of cropland NPP therefore must rely on census and survey data. However, these data  
60 report agricultural production, not NPP, and thus need crop-specific factors (dry  
61 matter fraction, harvest index, root to shoot ratio, etc.) to calculate the NPP (Gray et  
62 al., 2014; Huang et al., 2007; Monfreda et al., 2008; Prince et al., 2001), which  
63 neglected the temporal evolution for crop-specific factors such as harvest index and  
64 root to shoot ratio (Lorenz et al., 2010; Sinclair, 1998). Remote sensing by satellites is  
65 a powerful tool for estimating global terrestrial NPP (Cleveland et al., 2015; Field et  
66 al., 1995; Nemani et al., 2003; Parazoo et al., 2014; Zhao and Running, 2010), yet  
67 croplands are coincident with natural vegetation, making it difficult to differentiate  
68 the two using remote sensing (Defries et al., 2000; Monfreda et al., 2008).

69 The current state of the global carbon models is as follows: 1) some models, such  
70 as LPJ or ORCHIDEE, do not have an agricultural module; 2) models with an  
71 agricultural module, such as LPJ managed Land (LPJmL), do not fully represent the  
72 features of the Green Revolution; 3) the VEGAS model, by Zeng et al. (2014), was  
73 the first attempt to model the agricultural Green Revolution. The importance of  
74 parameter calibration has been recognized and addressed by numerous modelling  
75 studies (Bondeau et al., 2007; Chen et al., 2011; Crowther et al., 2016; Luo et al.,  
76 2016; Ogle et al., 2010; Peng et al., 2013). In addition, regional calibrated parameters  
77 are critical for global-scale modelling (Le Quéré et al., 2016). However, because the  
78 management data needed for most terrestrial models is spatially and temporally scarce,  
79 a precise regional simulation and calibration seems impossible (Bondeau et al., 2007).

80 Here, we conducted a study concentrated on calibrations at both the regional and  
81 the country scale. Instead of using an extensive set of actual management data that are  
82 unavailable or incomplete, we modelled the first-order effects on crop NPP using  
83 parameterizations. Our objectives were to 1) describe the method for simulating the



84 three Green Revolution features, 2) quantify the cropland NPP over the last fifty years  
85 on both the continental and country scales, and 3) improve the model's performance  
86 by key parameterization.

## 87 **2 Materials and methods**

### 88 **2.1 Simulating the Green Revolution with a dynamic vegetation model**

89 We simulated agriculture using a generic crop functional type that represents an  
90 average of three dominant crops: maize, wheat and rice. These crops are similar to  
91 warm C3 grass, one of the natural plant functional types in VEGAS (Zeng et al.,  
92 2005a; Zeng et al., 2014). A major difference is the narrower temperature growth  
93 function, to represent a warmer temperature requirement than natural vegetation.  
94 Cropland management is modelled as an enhanced photosynthetic rate by the cultivar  
95 selection, irrigation and application of fertilizers and pesticides. We modelled the  
96 first-order effects on carbon cycle using regional-scale parameterizations with the  
97 following rules.

#### 98 **2.1.1 Variety**

99 The selection of high-yield dwarf crop varieties has been a key feature of the  
100 agricultural Green Revolution since the 1960s, generally accompanied by an increase  
101 in the harvest index (the ratio of grain to aboveground biomass) (Sinclair, 1998). The  
102 harvest index (HI) varies for different crops, with a lower value for wheat (0.37-0.43)  
103 (Huang et al., 2007; Prince et al., 2001; Soltani et al., 2004) and higher values for rice  
104 (0.42-0.47) (Prasad et al., 2006; Witt et al., 1999) and maize (0.44-0.53) (Huang et al.,  
105 2007; Prince et al., 2001). We used a value of 0.45 for the year 2000, a typical value  
106 of the three major crops: maize, rice and wheat (Haberl et al., 2007; Sinclair, 1998).  
107 The temporal change of HI is modelled as:

$$108 \quad HI_{crop} = 0.45(1 + 0.6 \tanh(\frac{y-2000}{70})) \quad (1)$$

109 so that  $HI_{crop}$  was 0.31 at the beginning of the Green Revolution in 1961, and 0.45 for



110 2000 (Fig. 1), based on values found in the literature (Prince et al., 2001; Sinclair,  
111 1998).

### 112 **2.1.2 Irrigation**

113 To represent the effect of irrigation, the soil moisture function ( $\beta = w_1$  for  
114 unmanaged grass, where  $w_1$  is surface soil wetness) is modified as:

$$115 \quad \beta = 1 - \frac{(1-w_1)}{W_{\text{irrg}}} \quad (2)$$

116 The irrigation intensity  $W_{\text{irrg}}$  varies spatially from 1 (no irrigation) to 1.5 (high  
117 irrigation), with  $\beta$  ranging from 0 (no irrigation) to 0.33 (high irrigation) under  
118 extreme dry natural conditions (Fig. 2). This function also modifies  $\beta$  when  $w_1$  is not  
119 zero, but the effect of irrigation decreases when  $w_1$  increases and levels off when  $w_1$   
120 equals 1 (soil is saturated). Thus,  $\beta$  (and thus the photosynthesis rate) is determined by  
121 both naturally available water ( $w_1$ ) and irrigation. The spatial variation in  $W_{\text{irrg}}$  reflects  
122 a regional difference between tropical and temperate climates.

### 123 **2.1.3 Fertilizer and pesticide**

124 To represent the enhanced productivity from cultivar and fertilization, the gross  
125 carbon assimilation rate is modified by a management intensity factor (MI) that varies  
126 spatially and changes over time:

$$127 \quad MI(\text{region}, \text{year}) = M_0 M_1(\text{region}, MAT(\text{lat}, \text{lon})) M_2(\text{year}) \quad (3)$$

$$128 \quad M_1(\text{region}, MAT) = M_{1r}(\text{region}) * \text{Max}(1 - \tanh(MAT(\text{lat}, \text{lon}) - 15/25), 1.0) \quad (4)$$

$$130 \quad M_2(\text{year}) = 1 + 0.2 \tanh\left(\frac{\text{year} - 2000}{70}\right) \quad (5)$$

131 where  $M_0$  is a scaling factor, the default value taken as 1.7 compared with natural  
132 vegetation 1.0, while  $M_1$  is the spatially varying parameter, using major global regions  
133 as listed in Table 2 and mean annual temperature (MAT) to differentiate (Eq. 2).  $M_{1r}$  is  
134 a region-dependent relative management intensity factor and  $M_1$  is stronger in  
135 temperate and cold regions and weaker in tropical countries, for which we used the  
136 mean annual temperature as a surrogate (Eq. 2).  $M_2$  is a temporal evolutionary factor



137 (Eq. 3), and the term in parentheses represents the temporal evolution, modelled by a  
138 hyperbolic tangent function, with the MI values in 1961 approximately 10 % lower  
139 than in 2000, and 20 % lower asymptotically farther back in time (Fig. 3).

#### 140 **2.1.4 Motivation of the $M_{1r}$ parameter calibration**

141  $M_{1r}$  is a region-dependent relative management intensity factor that varied largely  
142 across regions, and the default parameters were derived from a previous version used  
143 in Zeng et al. (2014), mainly to capture the global trends, which neglected the  
144 regional trends to some degree. A main focus of this study is to improve the  $M_{1r}$   
145 parameter based on the FAO regional data to capture the regional trends. For each  
146 individual region, we used a series of parameters to drive the model and chose the  
147 best fit for the FAO statistical data (by naked eye observation) as follows:

- 148 1. Parameter  $M_{1r}$  was calibrated on a continental scale to match the FAO statistical  
149 data. During this period, countries within the same continent were assigned the  
150 same  $M_{1r}$ .
- 151 2. The  $M_{1r}$  for selected major countries was calibrated independently from the  
152 continental calibration, while the other countries that were not selected within the  
153 same continent were tuned oppositely from the selected countries to keep the total  
154 simulated continental production close to the FAO data.

155 After the two steps, total production was summed as all countries with updated  
156 parameters.

#### 157 **2.1.5 Planting, harvesting, and lateral transport**

158 Crop phenology was not decided beforehand but was determined by the climate  
159 condition. For example, when it is sufficiently warm in temperate and cool regions,  
160 crops begin to grow. This assumption captures most of the spring planting, and  
161 simulates multiple cropping in low latitudes. However, one limitation of such simple  
162 assumption is that it misses some other crop types, such as winter wheat, which has an  
163 earlier growth and harvest.



164 When the leaf area index (LAI) growth rate slows to a threshold value, a crop is  
165 assumed to be mature and is harvested. The automatical planting and harvest criteria  
166 allow multiple cropping in some warm regions, and matches areas with intense  
167 agriculture such as East Asia and Southeast Asia, but the criteria may overestimate  
168 regions with single cropping. Consequently, the simulated results tend to be the  
169 potential productivity due to the climate characteristics and our generic crop.

170 After harvest, grain and straw are assumed to be appropriated by farmers and then  
171 incorporated into the soil metabolic carbon pool. The harvested crop is redistributed  
172 according to population density, resulting in the horizontal transport of carbon. As a  
173 consequence, cropland areas act as net carbon sinks, and urban areas release large  
174 amount of CO<sub>2</sub> through heterotrophic respiration. Lateral transport is applied within  
175 each continent to simulate the first-order approximation. Additional information on  
176 cross-regional trade was also taken into account for eight major world economic  
177 regions.

## 178 **2.2 Data sets**

### 179 **Climate data**

180 Gridded monthly climate data sets (i.e., maximum and minimum temperature,  
181 precipitation, and radiation) covering the period 1901–2013 with a spatial resolution  
182 of 0.5°×0.5° were obtained from the Climatic Research Unit, University of East  
183 Anglia (<http://www.cru.uea.ac.uk/cru/data/hrg/>). The CRU TS3.22 (Harris et al., 2013)  
184 are calculated on high-resolution grids, which are based on an archive of monthly  
185 mean temperatures provided by more than 4000 weather stations distributed around  
186 the world. The dataset has been widely used for global change studies (Mitchell et al.,  
187 2004; Mitchell and Jones, 2005).

### 188 **Land-cover data**

189 The land-cover data set (crop/pasture versus natural vegetation) was derived from  
190 the History Database of the Global Environment (HYDE) data set  
191 (<http://themasites.pbl.nl/tridion/en/themasites/hyde/download/index-2.html>)





192 (Goldewijk et al., 2010; Goldewijk et al., 2011). It is an update of the HYDE with  
193 estimates of some of the underlying demographic and agricultural driving factors  
194 using historical population, cropland and pasture statistics combined with satellite  
195 information and specific allocation algorithms. The 3.1 version has a 5'  
196 longitude/latitude grid resolution, and covers the period 10,000 BC to AD 2000. This  
197 data set was also used in TRENDY and other model comparison projects (Chang et al.,  
198 2017; Sitch et al., 2015). The VEGAS model does not use high spatial resolution  
199 land-use and management data such as crop type and harvest practices; thus,  
200 small-scale regional patterns may not be well simulated, and the results are more  
201 reliable at aggregated continental to global scales.

#### 202 **Crop production data**

203 Crop production and cropland area are aggregated from FAO statistics for the major  
204 crops (FAOSTAT, <http://www.fao.org/faostat/en/#data/QC>, accessed June 2016).  
205 Specifically, they are the sum of the cereals (wheat, maize, rice, and barley, etc.) and  
206 five other major crops (cassava, oil palm, potatoes, soybean and sugar-cane), which  
207 comprise 90 % of the global amount of carbon harvested. Following Ciais et al.  
208 (2007), conversion factors are used to convert first wet to dry biomass, then to carbon  
209 content. The final conversion factors from wet biomass to carbon are 0.41 for cereals,  
210 0.57 for oil palm, 0.11 for potatoes, 0.08 for sugarcane, and 0.41 for soybean and  
211 cassava.

#### 212 **2.3 Initialization and simulation**

213 The VEGAS model used in TRENDY (Sitch et al., 2015; Zeng et al., 2005a) was  
214 run from 1700 to 2010 and, forced by climate, annual mean CO<sub>2</sub>, and land-use and  
215 management history. Due to unavailable data of observed climate data before 1900,  
216 the average climate data over the period from 1900 to 1909 was used to drive the  
217 “spin-up”. The VEGAS model has a speed up procedure for soil carbon to make it  
218 achieve equilibrium state (Zeng et al., 2005).



## 219 **3 Results**

### 220 **3.1 A brief revisit of the agricultural Green Revolution**

221 The agricultural Green Revolution was mostly started in the 1960s to cope with the  
222 food–population balance, particularly in developing countries (Borlaug, 2002) (Table  
223 1). Its features include the development of high-yield varieties (HYVs) of cereal  
224 grains, the expansion of irrigation, and applications of synthetic fertilizers and  
225 pesticides (Borlaug, 2007). The intensity of such management varies widely and has  
226 not always occurred synchronously in different parts of the world. Specifically, in the  
227 1950s, new wheat and maize varieties were developed by the International Maize and  
228 Wheat Improvement Center (CIMMYT) in Mexico, and their agricultural productivity  
229 increased with irrigated cultivation in the northwest (Byerlee and Moya, 1993; Gollin,  
230 2006; Pingali, 2012). Later in 1966, a new dwarf high-yield rice cultivar, IR8 was  
231 bred by the International Rice Research Institute (IRRI) in the Philippines, and it was  
232 spread and grown in most of the rice-growing countries of Asia, Africa and Latin  
233 America (Fischer et al., 1998; Khush, 2001; Peng et al., 1999). Also in the 1960s,  
234 India imported new wheat seed from CIMMYT to Punjab and later adopted IR8 rice  
235 variety from Philippines that could produce more grains (Parayil, 1992). China began  
236 participating in the Green Revolution in the 1970s, with hybrid rice bred by Longping  
237 Yuan (Yuan, 1966), and the fertilizer application rate increased dramatically from 43  
238 kg/ha in 1970 to 346 kg/ha in 1995 (Hazell, 2009). Meanwhile, Brazil began  
239 participating in the Green Revolution in the 1970s, and in collaboration with  
240 CIMMYT, high-yielding wheat varieties with aluminum toxicity resistance were  
241 developed, which were efficient in dealing with the aluminum toxicity in the Cerrado  
242 soils of Brazil (Davies, 2003; Khush, 2001). In contrast, African countries began their  
243 participation in the Green Revolution much later in the 1980s, with many obstacles  
244 from both climatic, edaphic and social-economic factors (Ejeta, 2010; Sánchez, 2010)  
245 and it featuring sustainable agriculture, plant breeding, and biotechnology.



246 **3.2 Global and continental comparison between model simulation and FAO**  
247 **statistical data**

248 Worldwide, the FAO data showed that cropland production increased from 439 TgC  
249 in 1961 to 1519 TgC in 2010 (246 % increase) (Fig. 4), and the VEGAS model  
250 captured most of this trend in both the default and the calibrated results. East Asia and  
251 North America contributed the most to this trend (Fig. 5). For East Asia, crop  
252 production increased from 65 TgC in 1961 to 342 TgC (426 % increase) in 2010. For  
253 North America, it increased from 90 TgC in 1961 to 235 TgC (161 % increase) in  
254 2010. Other regions followed the increasing trend except for the former USSR region.  
255 The lowest crop production existed in Central-West Asia and Oceania, with less than  
256 50 TgC over the study period.

257 As described in Sect. 2.1.4, we calibrated the  $M_{1r}$  parameter for each region. The  
258 default and updated regional management intensity parameter (Table 2) produced  
259 dramatically different estimations for some continents, for example in North America,  
260 Southeast Asia and Oceania (Fig. 5b, e, j). However, for other continents, such as  
261 South Asia, the improvement was not so pronounced. For East Asia, the default  
262 parameter was sufficient to capture most of the crop production variations. Moreover,  
263 the timing and magnitude of the agricultural Green Revolution was quite different  
264 over different regions. For example, it occurred more recently in Africa and South  
265 America (Fig. 5a,c) and much earlier in East Asia and Europe (Fig. 5d, i). In the  
266 region of former USSR, crop production even decreased after 1990 (Fig. 5h) due to  
267 the large areas of abandoned croplands, thus making the regional-scale simulation  
268 more complicated.

269 Furthermore, the updated parameters in different regions did not substantially  
270 change the total production estimations (Fig. 4), indicating that a good agreement in  
271 global total production may be overestimated in some regions while underestimated in  
272 others, which does not reflect the true nature of the production distributions and  
273 variations.



274 **3.3 Country-scale comparison between model simulation and FAO statistical**  
275 **data**

276 At the country level, the FAO data showed that China, the USA and India were the  
277 top three countries contributing to global crop production (Fig. 6). For China, crop  
278 production increased from 50 TgC in 1961 to 230 TgC in 2010 (360 % increase). For  
279 the USA, it increased from 76 TgC in 1961 to 204 TgC in 2010 (168 % increase).  
280 Other countries followed the same increasing trend with different rates. The lowest  
281 crop production in the top 9 countries existed in Canada and Argentina, with less than  
282 50 TgC over the study period.

283 As for the VEGAS simulations, the default parameters (Table 3) might  
284 overestimate results in some countries while underestimating others. The calibrated  
285 parameter could capture variations in most of the countries (Fig. 6). For Chinese crop  
286 production, a decreasing trend after 1999 was captured, but the magnitude was weaker  
287 (Fig. 6a), because the drop in cropland area was not represented in HYDE 3.0 for  
288 China. The calibrated parameter also performed well in other countries. For Brazil  
289 and Argentina, the dramatic increase after 2000 was not well captured due to the  
290 simple assumption that the strongest management occurred in 2000 and became  
291 weaker afterwards.

292 Based on the country-scale comparisons between the updated VEGAS simulations  
293 and the FAO statistical data of the decadal means, the linear regression slope was 1.00,  
294 with a higher  $R^2$  of 0.97 ( $p < 0.01$ ), a smaller RMSE of 10.5 TgC (~45 % decrease),  
295 and a smaller RMD of 3.5 TgC (~31 % decrease) compared with the default results  
296 (Fig. 7).

297 **3.4 Spatial comparison between the model simulation and the documented data**

298 The two independent datasets produced similar spatial distributions of crop NPP  
299 (Fig. 8). The highest crop NPP regions were the Great Plains of North America and  
300 temperate western Europe and East Asia ( $> 1.0$  Tg per  $0.5^\circ$  grid cell, Fig. 8), where the  
301 agricultural Green Revolution was the strongest, but high yields were also present



302 locally within tropical regions (e.g., Southeast Asia), while the lowest production in  
303 Africa, Eastern Europe and Russia ( $< 0.4 \text{ Tg per } 0.5^\circ$  grid cell, Fig. 8) was due largely  
304 to the low input in agricultural R & D and the rigid climate and edaphic conditions.  
305 The model result overestimated Russian cropland NPP because of the simplified  
306 model representation of temporal changes, and the abandoned cropland after the  
307 collapse of former USSR was not represented in the HYDE data set. Meanwhile, the  
308 high South American NPP was underestimated.

309 The average cereal NPP increased from  $1.0 \text{ Mg ha}^{-1}$  to  $1.5 \text{ Mg ha}^{-1}$  for African  
310 croplands (Fig. 9a), and it increased from  $1.5$  to  $2.1 \text{ Mg ha}^{-1}$  for Oceania croplands  
311 from 1961 to 2014. Europe, Asia and South America showed similar increasing trends  
312 from  $1.5$  to  $4.0 \text{ Mg ha}^{-1}$ . North America showed the highest cereal NPP, with an  
313 increase of  $2.5$  to  $8.0 \text{ Mg ha}^{-1}$  over the fifty years. For soybean NPP, America topped  
314 the six continents with  $3.0 \text{ Mg ha}^{-1}$  in 2010, while Africa showed the lowest NPP with  
315  $1.2 \text{ Mg ha}^{-1}$  in 2010, one-third that of America. Europe and Oceania had a middle  
316 level of  $\sim 2.0 \text{ Mg ha}^{-1}$  in 2010. This NPP trend was consistent with the progress of the  
317 Green Revolution progress on each continent.

#### 318 **4 Discussion**

319 In the estimation of crop NPP, one of the sources of uncertainty is crop parameters,  
320 such as variations in harvest index. When accounting for this variation of 0.45  
321 (0.37-0.53, or 18 % of the mean), the uncertainty resulted from the harvest index for  
322 the FAO production derived NPP would be  $1.3 \pm 0.2$  and  $3.6 \pm 0.6 \text{ PgC yr}^{-1}$  in the  
323 1960s and 2010s, respectively. Additionally, one of the main driving factors for the  
324 agricultural Green Revolution was the economic input. Gross domestic expenditures  
325 on food and agricultural R&D worldwide has increased from 27.4 to 65.5 billion of  
326 2009 purchasing power parity (PPP) dollars from 1980-2010 (Pardey et al., 2016).  
327 The middle-income countries R&D investment share increased from 29 % in 1980 to  
328 43 % in 2011. This investment difference has dramatically influenced the crop NPP  
329 (Fig. 4, 5, 6, 8) due to improvements in crop varieties, fertilizer and pesticide



330 application, and expansion of irrigation areas (Ejeta, 2010; Evenson, 2005; Evenson  
331 and Gollin, 2003; Gollin et al., 2005; Gray et al., 2014; Hazell, 2009). Despite a  
332 drought-induced reduction in the global terrestrial NPP of 0.55 PgC from 2000 to  
333 2009 based on MODIS satellite data analysis (Zhao and Running, 2010), cropland  
334 NPP increased 0.3-0.6 PgC for the same period in this study because of the  
335 agricultural Green Revolution (Fig. 4).

336 Gray et al. (2014) used production statistics and a carbon accounting model to show  
337 that increases in agricultural productivity explained ~25 % changes in atmospheric  
338 CO<sub>2</sub> seasonality. Northern Hemisphere extratropical maize, wheat, rice, and soybean  
339 production increased 0.33 PgC (240 %) between 1961 and 2008. This study showed a  
340 consistent estimation: the total cropland production increased 1.0 PgC (300 %), and  
341 took up 0.5 Pg more carbon in July. Furthermore, Monfreda et al. (2008) estimated the  
342 global cropland NPP for the year 2000 at the subcountry scale using the FAO  
343 statistical yield data and cropland area distributions. Consistently, the global cropland  
344 mean NPP was estimated as 4.2 MgC ha<sup>-1</sup>, with the highest NPP in Asian croplands of  
345 5.5 MgC ha<sup>-1</sup> and the lowest in African croplands of 2.5 MgC ha<sup>-1</sup>. Specifically, both  
346 studies agreed well in several regions that had the highest cultivated NPP due to  
347 intensive agriculture and/or multiple cropping: Western Europe; East Asia; the central  
348 United States; and southern Brazil, with NPP larger than 10 MgC ha<sup>-1</sup>. Meanwhile,  
349 Bondeau et al. (2007) modelled the difference of agricultural NPP between LPJmL  
350 and LPJ, showing that agriculture increased NPP in intensively managed or irrigated  
351 areas (Europe, China, southern United States, Argentina). However, their study could  
352 not capture the increasing trends in the US Central Plains and in the Australian wheat  
353 belt because of the unavailability of management data at those regional scales,  
354 showing the limitations of modelling using detailed regional management data.  
355 Moreover, using country-based agricultural statistics and activity maps of human and  
356 housed animal population densities, Ciais et al. (2007) estimated the global carbon  
357 harvested in croplands was 1.3 PgC yr<sup>-1</sup>, of which ~13 % enters into horizontal  
358 displacement through international trade circuits, contributing ~0.2-0.5 ppm mean  
359 latitudinal CO<sub>2</sub> gradients.



360 European cropland NPP increased 127 % over the last half century, as estimated by  
361 VEGAS (Fig. 5i), and the yield increased at a rate of 1.8 % per annum. Moreover,  
362 without the management intensity parameter updated, the crop yields for the 2000s  
363 would be 10.4 % lower. Similarly, a study showed that across all major crops  
364 cultivated in the EU, plant breeding has contributed approximately 74 % of total  
365 productivity growth since 2000, equivalent to a yield increase of 1.2 % per annum.  
366 European crop yields today would be more than 16 % lower without access to  
367 improved varieties (BSPB). The 2003 drought and heat in Europe reduced the  
368 terrestrial gross primary productivity (GPP) by 30 % (Ciais et al., 2005), while it was  
369 decreased by 15 % for cropland NPP in this study (Fig. 5i). This decrease was smaller  
370 than the natural ecosystem response due largely to the counteractive effects of  
371 management inputs (irrigation, fertilization, etc.).

372 In the central USA, VEGAS modelled the cropland NPP as  $> 6 \text{ MgC ha}^{-1}$  in the  
373 Great Plains and  $< 3 \text{ MgC ha}^{-1}$  in northwest and north USA for the 2000s. Prince et al.  
374 (2001) estimated crop NPP by applying crop-specific factors to statistical agricultural  
375 production. The NPP at the county-level in 1992 ranged from  $2 \text{ MgC ha}^{-1}$  in North  
376 Dakota, Wisconsin, and Minnesota to  $>8 \text{ MgC ha}^{-1}$  in central Iowa, Illinois, and Ohio.  
377 Areas of highest NPP were dominated by corn and soybean cultivation. Using a  
378 similar method, Hicke et al. (2004) estimated crop NPP increased in counties  
379 throughout the United States, with the largest increases occurring in the Midwest,  
380 Great Plains, and Mississippi River Valley regions. It was estimated that total  
381 coterminous cropland production increased from 0.37 to 0.53 (a 40 % increase)  $\text{Pg C}$   
382  $\text{yr}^{-1}$  during 1972–2001.

383 In Asian croplands, the percentage of harvested area for rice, wheat and maize  
384 under modern varieties was lower than 10 % in the 1960s, and it increased to over 80 %  
385 in the 2000s (Evenson, 2005). Moreover, nitrogen (N) fertilizer increased from  $23.9$   
386  $\text{kg ha}^{-1}$  in 1970 to  $168.6 \text{ kg ha}^{-1}$  in 2012, while the irrigated area increased from 25.2 %  
387 in 1970 to 33.2 % in 1995 (Rosegrant and Hazell, 2000). Correspondingly, the crop  
388 NPP increased from 1.4 in 1961 to  $4.5 \text{ MgC ha}^{-1}$  in 2014 (Fig. 9). Cropland NPP in  
389 China was estimated to increase from  $159 \text{ TgC yr}^{-1}$  in the 1960s to  $513 \text{ TgC yr}^{-1}$  in the



390 1990s based on the National Agriculture Database (Statistics Bureau of China 2000)  
391 (Huang et al., 2007), and this study estimated the range as 286 TgC yr<sup>-1</sup> in the 1960s  
392 to 559 TgC yr<sup>-1</sup> in the 1990s. In tropical Asia, the new croplands were mainly derived  
393 from forests, which caused large amounts of carbon losses from both vegetation and  
394 soil (Gibbs et al., 2010; Tao et al., 2013; West et al., 2010).

395 The African croplands currently nourish over 1.0 billion people. The need for  
396 sustainable agriculture combined with stable grain yield production is particularly  
397 urgent in Africa. However, the continent is now trading carbon for food. Newly  
398 cleared land in the tropics releases nearly 3 tons of carbon for every 1 ton of annual  
399 crop yield compared with a similar area cleared in the temperate zone (West et al.,  
400 2010). This continent can triple its crop yields provided the depletion of soil nutrients  
401 is addressed (Sánchez, 2010). Using chemical fertilizer as an example, the average N  
402 application rate from 2002 to 2012 was only ~14 kg ha<sup>-1</sup> yr<sup>-1</sup> in Africa, which severely  
403 hampered crop production (Han et al., 2016). In addition, complete crop residue  
404 removal for fodder and fuel is a norm in Africa, causing soils in these areas to lack  
405 organic matter input and to become carbon sources (Lal, 2004). Since the mid-1970s,  
406 ~50 Mha of Ethiopian land had no or low fertilizer application, resulting in low crop  
407 NPP (< 2 MgC ha<sup>-1</sup>, Fig. 7, 8) (West et al., 2010) and soil degradation (Shiferaw et al.,  
408 2013). African agricultural development has to overcome a series of constraints such  
409 as drought, poor soil fertility, diverse agro-ecologies, unique pests and diseases, and  
410 persistent institutional and programmatic challenges (Ejeta, 2010).

411 In terms of the data gap in management intensity, very few data sets provide  
412 long-term time series data with high spatial resolution. HYDE is a land use dataset  
413 that does not provide management intensity information (Goldewijk et al., 2011).  
414 Monfreda et al. (2008) developed a data set consisting of 175 crops consistent to the  
415 FAO statistical data for the period around year 2000. Moreover, Fritz et al. (2015)  
416 developed a cropland percentage map for the baseline year 2005. For the fertilizer  
417 dataset, Potter et al. (2010) provided the global manure N and P application rate for a  
418 mean state around year 2000. Moreover, Lu and Tian (2017) developed a global time  
419 series gridded data set for synthetic N and phosphorous (P) fertilizer application rate





420 in agricultural lands. For the irrigation data set, global monthly irrigated crop areas  
421 around the year 2000 were developed by Portmann et al. (2010). These data sets are  
422 mostly for a specific year or a period mean, and they are unsuitable for long-term  
423 simulations. Therefore, we still lack a comprehensive data set that reflects  
424 management intensity.

425 A more challenging task would be to calibrate regional parameters and explain  
426 spatial patterns better, because models may significantly underestimate the  
427 high-latitude trend (Graven et al., 2013) and overestimate elsewhere even if the global  
428 total is simulated correctly (Zeng et al., 2014). More work should be directed to  
429 reduce uncertainties in regional model parameterizations (Le Quéré et al., 2015; Luo  
430 et al., 2016). This paper focuses on both the continental and country scales to calibrate  
431 key parameters to better constrain the future projections of global cropland NPP.

## 432 **5 Conclusion**

433 We used a process-based terrestrial model VEGAS to simulate global cropland  
434 production from 1960 to 2010, and adapted the management intensity parameter at  
435 both continental and country scales. The updated parameter could capture the  
436 temporal dynamics of crop NPP much better than the default ones. The results showed  
437 that cropland NPP tripled from  $1.3 \pm 0.1$  in the 1960s to  $3.6 \pm 0.2$  Pg C yr<sup>-1</sup> in the  
438 2000s. The NPP increased most notably in the U.S. Midwest, Western Europe and the  
439 North China Plain. In contrast, it increased slowly in Africa and Oceania. We  
440 highlight the large difference in model parameterization among regions when  
441 simulating the crop NPP due to the differences in timing and magnitude of the Green  
442 Revolution. To better explain the history and predict the future crop NPP trends, it is  
443 important to calibrate key parameters at regional scales and develop time series data  
444 sets for land management history.



## 445 References:

- 446 Bondeau, A., Smith, P. C., Zaehle, S., Schaphoff, S., Lucht, W., Cramer, W., Gerten, D., Lotze-Campen,  
447 H., MÜLLER, C., Reichstein, M., and Smith, B.: Modelling the role of agriculture for the 20th  
448 century global terrestrial carbon balance, *Global Change Biology*, 13, 679-706, 2007.
- 449 Borlaug, N.: Feeding a hungry world, *Science*, 318, 359-359, 2007.
- 450 Borlaug, N. E.: The green revolution revisited and the road ahead, Nobelprize.org, 2002.
- 451 BSPB: EU study highlights benefits of plant breeding. Plant Breeding Matters. the British Society of  
452 Plant Breeders.  
453 [http://www.bspb.co.uk/sg\\_userfiles/BSPB\\_Plant\\_Breeding\\_Matters\\_Spring\\_2016.pdf](http://www.bspb.co.uk/sg_userfiles/BSPB_Plant_Breeding_Matters_Spring_2016.pdf), last  
454 access: May 2017.
- 455 Byerlee, D. and Moya, P.: Impacts of International Wheat Breeding Research in the Developing World,  
456 *Wheats*, 1993. 1993.
- 457 Chang, J., Philippe, C., Xuhui, W., Shilong, P., Ghassem, A., Richard, B., Frédéric, C., Marie, D., Louis,  
458 F., Katja, F., Anselmo García Cantú R., Alexandra-Jane, H., Thomas, H., Akihiko, I., Catherine,  
459 M., Guy, M., Kazuya, N., Sebastian, O., Shufen, P., Shushi, P., Rashid, R., Christopher, R.,  
460 Christian, R., Sibyll, S., Jörg, S., Hanqin, T., Nicolas, V., Jia, Y., Ning, Z., and Fang, Z.:  
461 Benchmarking carbon fluxes of the ISIMIP2a biome models, *Environmental Research Letters*, 12,  
462 045002, 2017.
- 463 Chen, T., van der Werf, G. R., Dolman, A., and Groenendijk, M.: Evaluation of cropland maximum  
464 light use efficiency using eddy flux measurements in North America and Europe,  
465 *GEOPHYSICAL RESEARCH LETTERS*, 38, L14707, 2011.
- 466 Ciais, P., Bousquet, P., Freibauer, A., and Naegler, T.: Horizontal displacement of carbon associated  
467 with agriculture and its impacts on atmospheric CO<sub>2</sub>, *Global Biogeochemical Cycles*, 21, 776-786,  
468 2007.
- 469 Ciais, P., Reichstein, M., Viovy, N., Granier, A., Ogee, J., Allard, V., Aubinet, M., Buchmann, N.,  
470 Bernhofer, C., Carrara, A., Chevallier, F., De Noblet, N., Friend, A. D., Friedlingstein, P.,  
471 Grunwald, T., Heinesch, B., Keronen, P., Knohl, A., Krinner, G., Loustau, D., Manca, G.,  
472 Matteucci, G., Miglietta, F., Ourcival, J. M., Papale, D., Pilegaard, K., Rambal, S., Seufert, G.,  
473 Soussana, J. F., Sanz, M. J., Schulze, E. D., Vesala, T., and Valentini, R.: Europe-wide reduction in  
474 primary productivity caused by the heat and drought in 2003, *Nature*, 437, 529-533, 2005.
- 475 Cleveland, C. C., Taylor, P., Chadwick, K. D., Dahlin, K., Doughty, C. E., Malhi, Y., Smith, W. K.,  
476 Sullivan, B. W., Wieder, W. R., and Townsend, A. R.: A comparison of plot-based satellite and  
477 Earth system model estimates of tropical forest net primary production, *Global Biogeochemical*  
478 *Cycles*, 29, 626-644, 2015.
- 479 Crowther, T. W., Todd-Brown, K. E. O., Rowe, C. W., Wieder, W. R., Carey, J. C., Machmuller, M. B.,  
480 Snoek, B. L., Fang, S., Zhou, G., Allison, S. D., Blair, J. M., Bridgham, S. D., Burton, A. J.,  
481 Carrillo, Y., Reich, P. B., Clark, J. S., Classen, A. T., Dijkstra, F. A., Elberling, B., Emmett, B. A.,  
482 Estiarte, M., Frey, S. D., Guo, J., Harte, J., Jiang, L., Johnson, B. R., Kröel-Dulay, G., Larsen, K.  
483 S., Laudon, H., Lavallee, J. M., Luo, Y., Lupascu, M., Ma, L. N., Marhan, S., Michelsen, A.,  
484 Mohan, J., Niu, S., Pendall, E., Peñuelas, J., Pfeifer-Meister, L., Poll, C., Reinsch, S., Reynolds, L.  
485 L., Schmidt, I. K., Sistla, S., Sokol, N. W., Templer, P. H., Treseder, K. K., Welker, J. M., and  
486 Bradford, M. A.: Quantifying global soil carbon losses in response to warming, *Nature*, 540,



- 487 104-108, 2016.
- 488 Davies, W. P.: An Historical Perspective from the Green Revolution to the Gene Revolution, *Nutrition*
- 489 *Reviews*, 61, S124-134, 2003.
- 490 Defries, R. S., Hansen, M. C., Townshend, J. R. G., Janetos, A. C., and Loveland, T. R.: A new global
- 491 1-km dataset of percentage tree cover derived from remote sensing, *Global Change Biology*, 6,
- 492 247-254, 2000.
- 493 Ejeta, G.: African Green Revolution needn't be a mirage, *Science*, 327, 831-832, 2010.
- 494 Evenson, R. E.: Besting Malthus: The Green Revolution, *Proceedings of the American Philosophical*
- 495 *Society*, 149, 469-486, 2005.
- 496 Evenson, R. E. and Gollin, D.: Assessing the impact of the Green Revolution, 1960 to 2000, *Science*,
- 497 300, 758-762, 2003.
- 498 Field, C. B., Randerson, J. T., and Malmström, C. M.: Global net primary production: Combining
- 499 ecology and remote sensing, *Remote Sensing of Environment*, 51, 74-88, 1995.
- 500 Fischer, K. S., Cordova, V. G., Pingali, P. L., and Hossain, M.: Impact of IRRI on rice science and
- 501 production, 1998. 27-50, 1998.
- 502 Foley, J. A., Ramankutty, N., Brauman, K. A., Cassidy, E. S., Gerber, J. S., Johnston, M., Mueller, N.
- 503 D., O'Connell, C., Ray, D. K., and West, P. C.: Solutions for a cultivated planet, *Nature*, 478,
- 504 337-342, 2011.
- 505 Fritz, S., See, L., McCallum, I., You, L., Bun, A., Moltchanova, E., Duerauer, M., Albrecht, F., Schill,
- 506 C., and Perger, C.: Mapping global cropland and field size, *Global change biology*, 21, 1980-1992,
- 507 2015.
- 508 Gibbs, H. K., Ruesch, A. S., Achard, F., Clayton, M. K., Holmgren, P., Ramankutty, N., and Foley, J. A.:
- 509 Tropical forests were the primary sources of new agricultural land in the 1980s and 1990s. *Proc*
- 510 *Natl Acad Sci USA*, *Proceedings of the National Academy of Sciences of the United States of*
- 511 *America*, 107, 16732-16737, 2010.
- 512 Glaeser, B.: *The Green Revolution revisited: critique and alternatives*, Taylor & Francis, 2010.
- 513 Goldewijk, K. K., Beusen, A., and Janssen, P.: Long term dynamic modeling of global population and
- 514 built-up area in a spatially explicit way: HYDE 3.1, *Holocene*, 20, 565-573, 2010.
- 515 Goldewijk, K. K., Beusen, A., van Drecht, G., and de Vos, M.: The HYDE 3.1 spatially explicit
- 516 database of human-induced global land-use change over the past 12,000 years, *Global Ecology*
- 517 *and Biogeography*, 20, 73-86, 2011.
- 518 Gollin, D.: *Impacts of International Research on Intertemporal Yield Stability in Wheat and Maize: An*
- 519 *Economic Assessment*, Impact Studies, 2006. 2006.
- 520 Gollin, D., Morris, M., and Byerlee, D.: Technology Adoption in Intensive Post-Green Revolution
- 521 Systems, *American Journal of Agricultural Economics*, 87, 1310-1316, 2005.
- 522 Graven, H. D., Keeling, R. F., Piper, S. C., Patra, P. K., Stephens, B. B., Wofsy, S. C., Welp, L. R.,
- 523 Sweeney, C., Tans, P. P., and Kelley, J. J.: Enhanced seasonal exchange of CO<sub>2</sub> by northern
- 524 ecosystems since 1960, *Science*, 341, 1085-1089, 2013.
- 525 Gray, J. M., Frohling, S., Kort, E. A., Ray, D. K., Kucharik, C. J., Ramankutty, N., and Friedl, M. A.:
- 526 Direct human influence on atmospheric CO<sub>2</sub> seasonality from increased cropland productivity,
- 527 *Nature*, 515, 398-401, 2014.
- 528 Haberl, H., Erb, K. H., Krausmann, F., Gaube, V., Bondeau, A., Plutzar, C., Gingrich, S., Lucht, W., and
- 529 Fischerkowsky, M.: Quantifying and mapping the human appropriation of net primary
- 530 production in earth's terrestrial ecosystems, *Proceedings of the National Academy of Sciences*,



- 531 104, 12942-12947, 2007.
- 532 Han, P., Zhang, W., Wang, G., Sun, W., and Huang, Y.: Changes in soil organic carbon in croplands  
533 subjected to fertilizer management: a global meta-analysis, *Scientific Reports*, 6, 27199, 2016.
- 534 Harris, I., Jones, P., Osborn, T., and Lister, D.: Updated high - resolution grids of monthly climatic  
535 observations—the CRU TS3. 10 Dataset, *International Journal of Climatology*, 34, 623-642, 2013.
- 536 Hazell, P. B.: *The Asian green revolution*, Intl Food Policy Res Inst, 2009.
- 537 Hicke, J. A., Lobell, D. B., and Asner, G. P.: Cropland Area and Net Primary Production Computed  
538 from 30 Years of USDA Agricultural Harvest Data, *Earth Interactions*, 8, 145-147, 2004.
- 539 Huang, Y., Zhang, W., Sun, W., and Zheng, X.: Net primary production of Chinese croplands from  
540 1950 to 1999, *Ecological Applications*, 17, 692-701, 2007.
- 541 Khush, G. S.: Green revolution: the way forward, *Nature Reviews Genetics*, 2, 815, 2001.
- 542 Lal, R.: Soil carbon sequestration impacts on global climate change and food security, *science*, 304,  
543 1623-1627, 2004.
- 544 Le Quéré, C., Andrew, R. M., Canadell, J. G., Sitch, S., Korsbakken, J. I., Peters, G. P., Manning, A. C.,  
545 Boden, T. A., Tans, P. P., Houghton, R. A., Keeling, R. F., Alin, S., Andrews, O. D., Anthoni, P.,  
546 Barbero, L., Bopp, L., Chevallier, F., Chini, L. P., Ciais, P., Currie, K., Delire, C., Doney, S. C.,  
547 Friedlingstein, P., Gkritzalis, T., Harris, I., Hauck, J., Haverd, V., Hoppema, M., Klein Goldewijk,  
548 K., Jain, A. K., Kato, E., Körtzinger, A., Landschützer, P., Lefèvre, N., Lenton, A., Lienert, S.,  
549 Lombardozi, D., Melton, J. R., Metzl, N., Millero, F., Monteiro, P. M. S., Munro, D. R., Nabel, J.  
550 E. M. S., Nakaoka, S. I., O'Brien, K., Olsen, A., Omar, A. M., Ono, T., Pierrot, D., Poulter, B.,  
551 Rödenbeck, C., Salisburly, J., Schuster, U., Schwinger, J., Sferián, R., Skjelvan, I., Stocker, B. D.,  
552 Sutton, A. J., Takahashi, T., Tian, H., Tilbrook, B., van der Laan-Luijkx, I. T., van der Werf, G. R.,  
553 Viovy, N., Walker, A. P., Wiltshire, A. J., and Zaehle, S.: Global Carbon Budget 2016, *Earth Syst.*  
554 *Sci. Data*, 8, 605-649, 2016.
- 555 Lorenz, A. J., Gustafson, T. J., Coors, J. G., and Leon, N. d.: Breeding Maize for a Bioeconomy: A  
556 Literature Survey Examining Harvest Index and Stover Yield and Their Relationship to Grain  
557 Yield, *Crop Science*, 50, 1-12, 2010.
- 558 Lu, C. and Tian, H.: Global nitrogen and phosphorus fertilizer use for agriculture production in the past  
559 half century: shifted hot spots and nutrient imbalance, *Earth System Science Data*, 9, 181, 2017.
- 560 Luo, Y., Ahlström, A., Allison, S. D., Batjes, N. H., Brovkin, V., Carvalhais, N., Chappell, A., Ciais, P.,  
561 Davidson, E. A., and Finzi, A.: Towards More Realistic Projections of Soil Carbon Dynamics by  
562 Earth System Models, *Global Biogeochemical Cycles*, 30, 40-56, 2016.
- 563 Mitchell, T. D., Carter, T. R., Jones, P. D., Hulme, M., and New, M.: A comprehensive set of  
564 high-resolution grids of monthly climate for Europe and the globe: the observed record  
565 (1901-2000) and 16 scenarios (2001-2100), Tyndall Centre for Climate Change Research Working  
566 Paper, 55, 25, 2004.
- 567 Mitchell, T. D. and Jones, P. D.: An improved method of constructing a database of monthly climate  
568 observations and associated high - resolution grids, *International journal of climatology*, 25,  
569 693-712, 2005.
- 570 Monfreda, C., Ramankutty, N., and Foley, J. A.: Farming the planet: 2. Geographic distribution of crop  
571 areas, yields, physiological types, and net primary production in the year 2000, *Global*  
572 *biogeochemical cycles*, 22, 2008.
- 573 Nemani, R. R., Keeling, C. D., Hashimoto, H., Jolly, W. M., Piper, S. C., Tucker, C. J., Myneni, R. B.,  
574 and Running, S. W.: Climate-Driven Increases in Global Terrestrial Net Primary Production from



- 575 1982 to 1999, *Science*, 300, 1560, 2003.
- 576 Ogle, S. M., BREIDT, F., Easter, M., Williams, S., Killian, K., and Paustian, K.: Scale and uncertainty  
577 in modeled soil organic carbon stock changes for US croplands using a process - based model,  
578 *Global Change Biology*, 16, 810-822, 2010.
- 579 Parayil, G.: *The Green Revolution in India: A Case Study of Technological Change, Technology &*  
580 *Culture*, 33, 737, 1992.
- 581 Parazoo, N. C., Bowman, K., Fisher, J. B., Frankenberg, C., Jones, D. B. A., Cescatti, A., Pérez-Priego,  
582 Ó., Wohlfahrt, G., and Montagnani, L.: Terrestrial gross primary production inferred from satellite  
583 fluorescence and vegetation models, *Global Change Biology*, 20, 3103-3121, 2014.
- 584 Pardey, P. G., Chan-Kang, C., Dehmer, S. P., and Beddow, J. M.: Agricultural R&D is on the Move,  
585 *Nature*, 537, 301-303, 2016.
- 586 Peng, S., Cassman, K. G., Virmani, S. S., Sheehy, J., and Khush, G. S.: Yield Potential Trends of  
587 Tropical Rice since the Release of IR8 and the Challenge of Increasing Rice Yield Potential, *Crop*  
588 *Science*, 39, 1552-1559, 1999.
- 589 Peng, S., Piao, S., Shen, Z., Ciais, P., Sun, Z., Chen, S., Bacour, C., Peylin, P., and Chen, A.:  
590 Precipitation amount, seasonality and frequency regulate carbon cycling of a semi-arid grassland  
591 ecosystem in Inner Mongolia, China: A modeling analysis, *Agricultural & Forest Meteorology*, s  
592 178–179, 46-55, 2013.
- 593 Pingali, P. L.: Green revolution: impacts, limits, and the path ahead, *Proceedings of the National*  
594 *Academy of Sciences of the United States of America*, 109, 12302, 2012.
- 595 Portmann, F. T., Siebert, S., and Döll, P.: MIRCA2000—Global monthly irrigated and rainfed crop  
596 areas around the year 2000: A new high - resolution data set for agricultural and hydrological  
597 modeling, *Global biogeochemical cycles*, 24, 2010.
- 598 Potter, P., Ramankutty, N., Bennett, E. M., and Donner, S. D.: Characterizing the spatial patterns of  
599 global fertilizer application and manure production, *Earth Interactions*, 14, 1-22, 2010.
- 600 Prasad, P. V. V., Boote, K. J., Allen, L. H., Sheehy, J. E., and Thomas, J. M. G.: Species, ecotype and  
601 cultivar differences in spikelet fertility and harvest index of rice in response to high temperature  
602 stress, *Field Crops Research*, 95, 398-411, 2006.
- 603 Prince, S. D., Haskett, J., Steininger, M., Strand, H., and Wright, R.: Net Primary Production of U.S.  
604 Midwest Croplands from Agricultural Harvest Yield Data, *Ecological Applications*, 11, 1194-1205,  
605 2001.
- 606 Rosegrant, M. W. and Hazell, P. B.: *Transforming the rural Asian economy: The unfinished revolution*,  
607 Oxford University Press Oxford, 2000.
- 608 Sánchez, P. A.: Tripling crop yields in tropical Africa, *Nature Geoscience*, 3, 299-300, 2010.
- 609 Shiferaw, A., Hurni, H., and Zeleke, G.: A Review on Soil Carbon Sequestration in Ethiopia to Mitigate  
610 Land Degradation and Climate Change, *J. Environ. Earth Sci.*, 3, 187-200, 2013.
- 611 Sinclair, T. R.: Historical changes in harvest index and crop nitrogen accumulation, *Crop Science*, 38,  
612 638-643, 1998.
- 613 Sitch, S., Friedlingstein, P., Gruber, N., Jones, S. D., Murraytortarolo, G., Ahlström, A., Doney, S. C.,  
614 Graven, H., Heinze, C., and Huntingford, C.: Recent trends and drivers of regional sources and  
615 sinks of carbon dioxide, *Biogeosciences*, 12, 653-679, 2015.
- 616 Soltani, A., Galeshi, S., Attarbashi, M. R., and Taheri, A. H.: Comparison of two methods for  
617 estimating parameters of harvest index increase during seed growth, *Field Crops Research*, 89,  
618 369-378, 2004.



- 619 Tao, B., Tian, H., Chen, G., Ren, W., Lu, C., Alley, K. D., Xu, X., Liu, M., Pan, S., and Virji, H.:  
620 Terrestrial carbon balance in tropical Asia: Contribution from cropland expansion and land  
621 management, *Global and Planetary Change*, 100, 85-98, 2013.
- 622 West, P. C., Gibbs, H. K., Monfreda, C., Wagner, J., Barford, C. C., Carpenter, S. R., and Foley, J. A.:  
623 Trading carbon for food: global comparison of carbon stocks vs. crop yields on agricultural land,  
624 *Proceedings of the National Academy of Sciences of the United States of America*, 107,  
625 19645-19648, 2010.
- 626 Witt, C., Dobermann, A., Abdulrachman, S., Gines, H. C., Guanghai, W., Nagarajan, R.,  
627 Satawatanont, S., Son, T. T., Tan, P. S., and Van, T. L.: Internal nutrient efficiencies of irrigated  
628 lowland rice in tropical and subtropical Asia, *Field Crops Research*, 63, 113-138, 1999.
- 629 Yuan, L. P.: Male sterility in rice, *Chinese Sci Bull*, 17, 185-188, 1966.
- 630 Zeng, N., Mariotti, A., and Wetzel, P.: Terrestrial mechanisms of interannual CO<sub>2</sub> variability, *Global*  
631 *Biogeochemical Cycles*, 19, n/a-n/a, 2005a.
- 632 Zeng, N., Qian, H., Roedenbeck, C., and Heimann, M.: Impact of 1998–2002 midlatitude drought and  
633 warming on terrestrial ecosystem and the global carbon cycle, *Geophysical Research Letters*, 32,  
634 2005b.
- 635 Zeng, N., Zhao, F., Collatz, G. J., Kalnay, E., Salawitch, R. J., West, T. O., and Guanter, L.:  
636 Agricultural Green Revolution as a driver of increasing atmospheric CO<sub>2</sub> seasonal amplitude,  
637 *Nature*, 515, 394-397, 2014.
- 638 Zhao, M. and Running, S. W.: Drought-induced reduction in global terrestrial net primary production  
639 from 2000 through 2009, *science*, 329, 940-943, 2010.
- 640
- 641

642 **Tables:**



643 Table 1 Features of the agricultural Green Revolution across regions

644

Region/Coun- try	Starting period	Features	Ref.
Africa	1980s	Sustainable agriculture, plant breeding, and biotechnology	(Evenson and Gollin, 2003); (Ejeta, 2010);(Pingali, 2012)
Asia	1960s	Varieties breeding, use of chemical fertilizers and pesticides, and irrigation	(Hazell, 2009)
Europe and North America	1960s	Large public investment in crop genetic improvement built on the scientific advances for the major staple crops —wheat, rice, and maize	(Pingali, 2012)
South America	1960s	Varieties breeding, use of chemical fertilizers and pesticides, and irrigation	(Evenson and Gollin, 2003); (Hazell, 2009)
Mexico	1950s	New wheat and maize varieties developed by the International Maize and Wheat Improvement Center. Improve agricultural productivity with irrigated cultivation in northwest	(Cotter, 2005); (Khush, 2001);(Pingali, 2012)
Philippines	1966	A new dwarfed high-yield rice cultivar, IR8 was bred by IRRI	(Fischer et al., 1998); (Peng et al., 1999)



---

India	1960s	Plant breeding, irrigation development, and financing of agrochemicals	(Hazell, 2009); (Yuan, 1966); (Lin and Yuan, 1980)
China	1970s	Hybrid rice bred by Longping Yuan; Fertilizer increased dramatically	(Davies, 2003);(Khush, 2001);(Marris, 2005)
Brazil	1970s	High-yielding wheat varieties with aluminum toxicity resistance were developed	





645 Table 2 Default and calibrated regional management intensity parameter of  $M_{1r}$ . The  
 646 default values were obtained from Zeng et al., (2014), which were parameterized  
 647 mainly for global trend simulation. See Sect. 2.1.4 for the calibration. Updated  $M_{1r}$   
 648 values are represented by  $\uparrow$  and  $\downarrow$  symbols, indicating an increase or a decrease  
 649 compared to the default ones, respectively.

Continent	Default	Calibrated
Africa	0.5	0.8 $\uparrow$
North America	1.3	1.1 $\downarrow$
South America	0.7	0.9 $\uparrow$
East Asia	1.5	1.5
Southeast Asia	1.0	0.7 $\downarrow$
South Asia	0.7	0.6 $\downarrow$
Central-West Asia	0.7	1.0 $\uparrow$
Former USSR	1.0	1.2 $\uparrow$
Rest of Europe	1.3	1.1 $\downarrow$
Oceania	1.0	0.6 $\downarrow$

650

651 Table 3 Default and calibrated national management intensity parameter of  $M_{1r}$ .

Country	Default	Calibrated
China	1.5	1.3 $\downarrow$
USA	1.3	1.0 $\downarrow$
India	0.7	0.6 $\downarrow$
Russia	1.0	0.9 $\downarrow$
Brazil	0.7	0.8 $\uparrow$
Indonesia	1.0	0.7 $\downarrow$
France	1.3	3.0 $\uparrow$
Canada	1.3	2.1 $\uparrow$
Argentina	0.7	0.8 $\uparrow$

652



653 **Figure Captions:**

654 Figure 1: Harvest index change over time as used in the model, and a harvest index of  
655 0.31 in 1961 and 0.49 in 2010, based on literature review.

656 Figure 2: Irrigation intensity ( $W_{\text{irrig}}$ ) changes with mean annual temperature (MAT)  
657 and  $\beta$  (beta) changes with soil wetness for typical  $W_{\text{irrig}}$  as used in the model.

658 Figure 3: Management intensity (relative to year 2000) changes over time as used in  
659 the model. The analytical functions are hyperbolic tangent (see text). The parameter  
660 values correspond to a management intensity in 1961 that is 10 % smaller than in  
661 2010.

662 Figure 4: Annual global crop production from 1961 to 2010. Default parameters were  
663 derived from a previous version that was used in Zeng et al., (2014) to capture the  
664 global trends, and calibrated parameters were set in this study (see text) to capture the  
665 regional trends.

666 Figure 5: Annual crop production from 1961 to 2010 at continental scales. The (d)  
667 subplot has no purple line since the default parameter produced the best fit for all the  
668 tuned simulations.

669 Figure 6: Annual crop production from 1961 to 2010 at country scales.

670 Figure 7: Country-based comparison of simulated and observed cropland productions  
671 ( $T_g$ ) before (a) and after (b) calibration. Each country consists of five dots  
672 representing the five decadal mean values, respectively.

673 Figure 8: Mean cropland NPP from 1997 to 2003. VEGAS modelled patterns (in units  
674 of  $T_g$  C per  $0.5^\circ$  grid cell, upper panel) show major productions in the agricultural  
675 areas of North America, Europe and Asia (the lower panel shows the mean crop NPP  
676 based on the FAO statistical data from Navin Ramankutty (<http://www.earthstat.org/>)).

677 Figure 9: Cereal and soybean NPP at continental scales over the last 60 years derived  
678 from FAO yield data. Note that the scales are different.

679

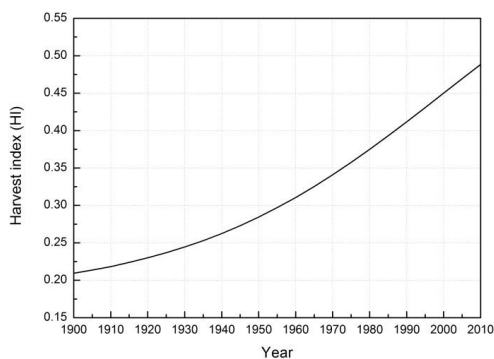
680

681



682

683

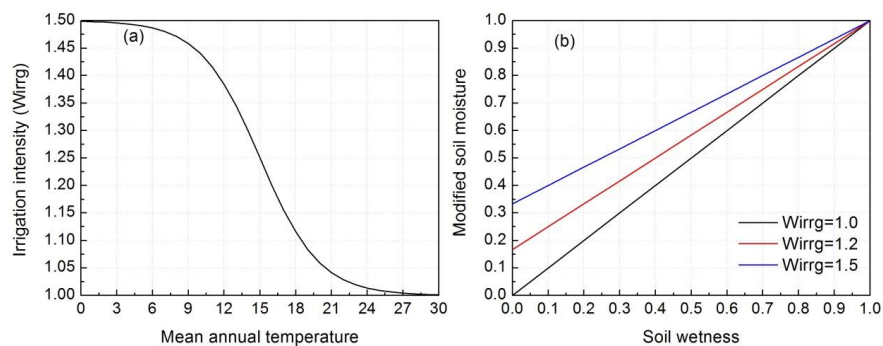


684

685 Figure 1: Harvest index change over time as used in the model, and a harvest index of  
686 0.31 in 1961 and 0.49 in 2010, based on literature review.

687

688

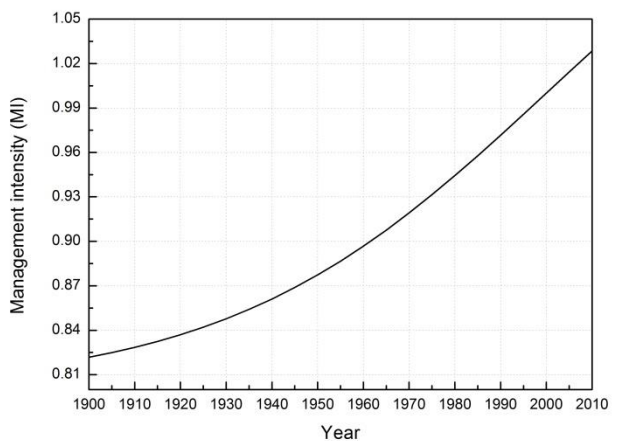


689

690 Figure 2: Irrigation intensity ( $W_{\text{irrig}}$ ) changes with mean annual temperature (MAT)  
691 and  $\beta$  (beta) changes with soil wetness for typical  $W_{\text{irrig}}$  as used in the model.

692

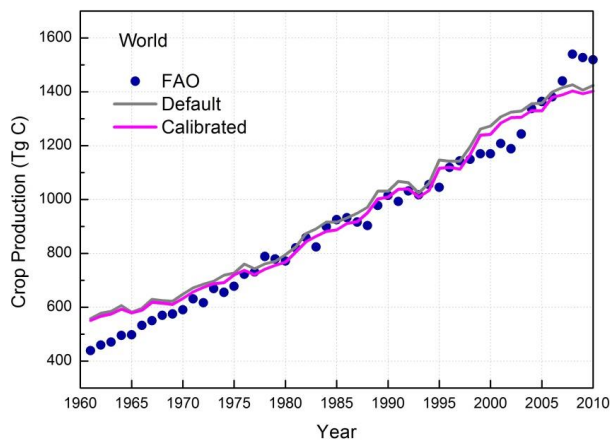
693



694

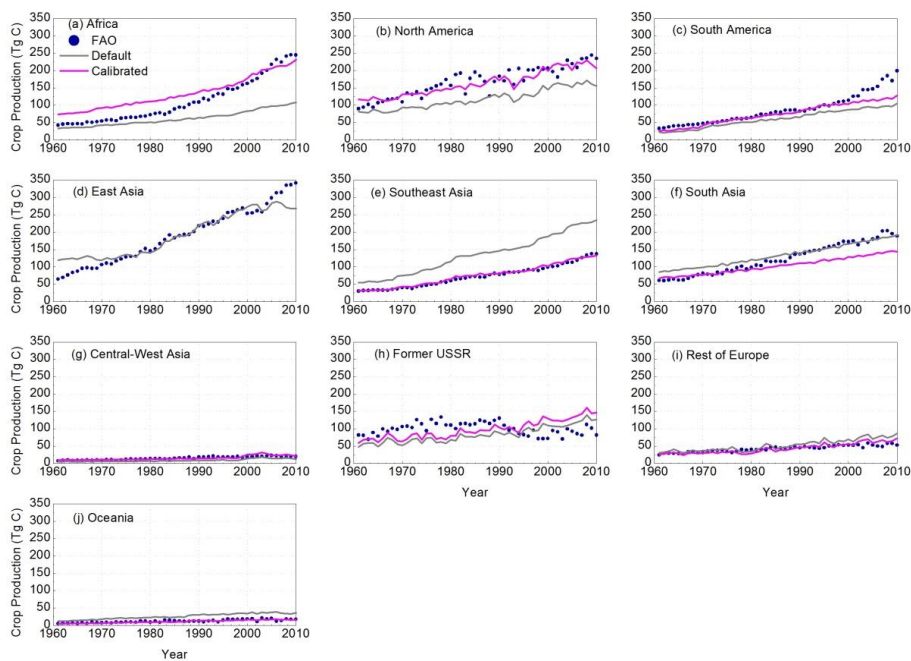
695 Figure 3: Management intensity (relative to year 2000) changes over time as used in  
696 the model. The analytical functions are hyperbolic tangent (see text). The parameter  
697 values correspond to a management intensity in 1961 that is 10 % smaller than in  
698 2010.

699



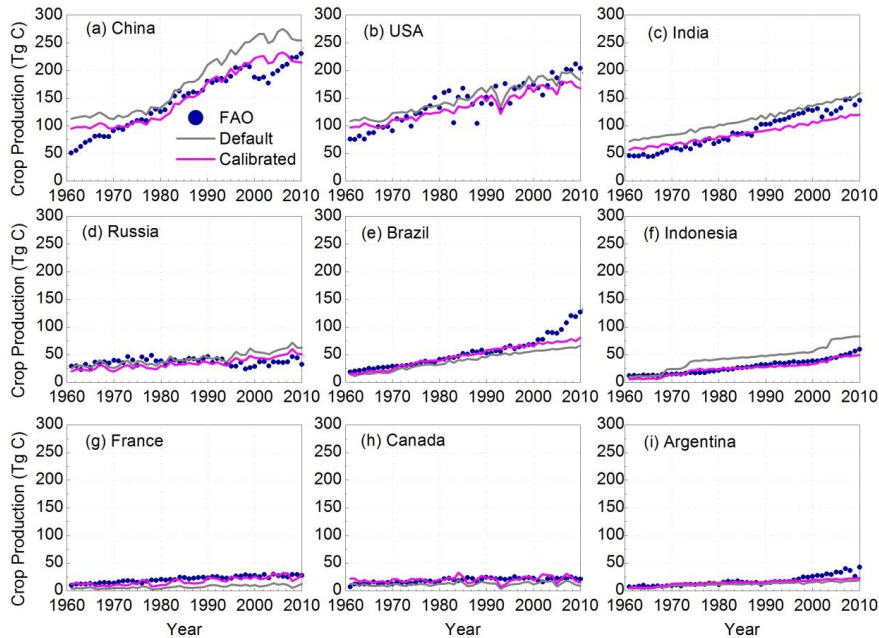
700

701 Figure 4: Annual global crop production from 1961 to 2010. Default parameters were  
702 derived from a previous version that was used in Zeng et al., (2014) to capture the  
703 global trends, and calibrated parameters were set in this study (see text) to capture the  
704 regional trends.



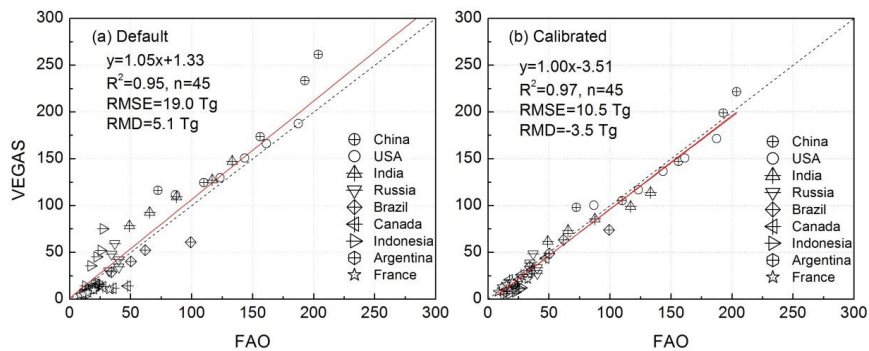
705

706 Figure 5: Annual crop production from 1961 to 2010 at continental scales. The (d)  
707 subplot has no purple line since the default parameter produced the best fit for all the  
708 tuned simulations.



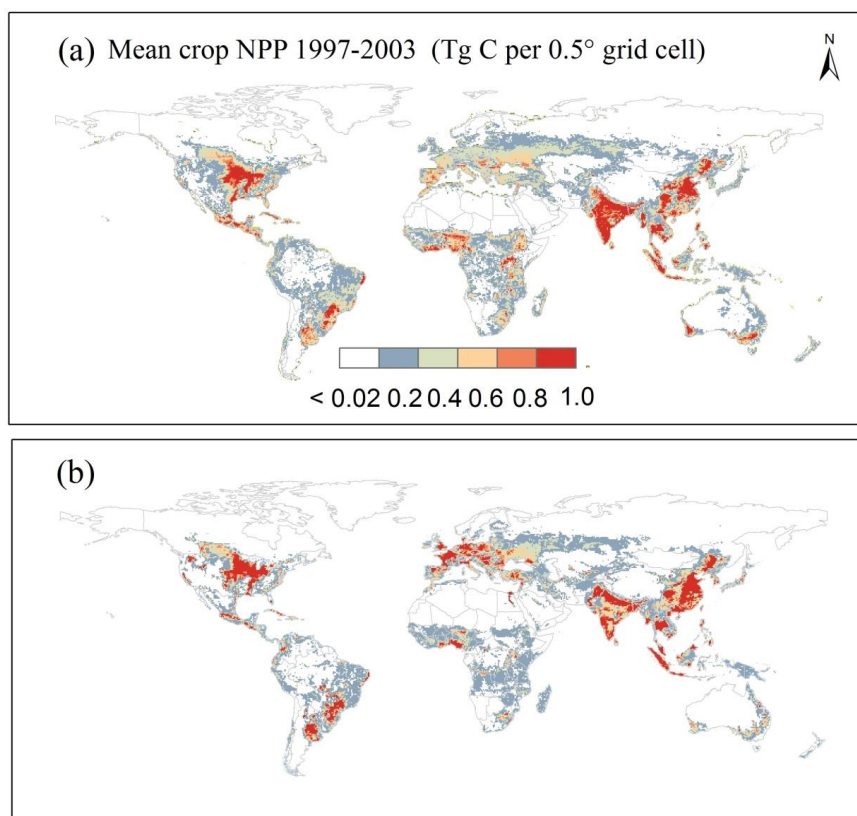
709  
 710  
 711  
 712

Figure 6: Annual crop production from 1961 to 2010 at country scales.

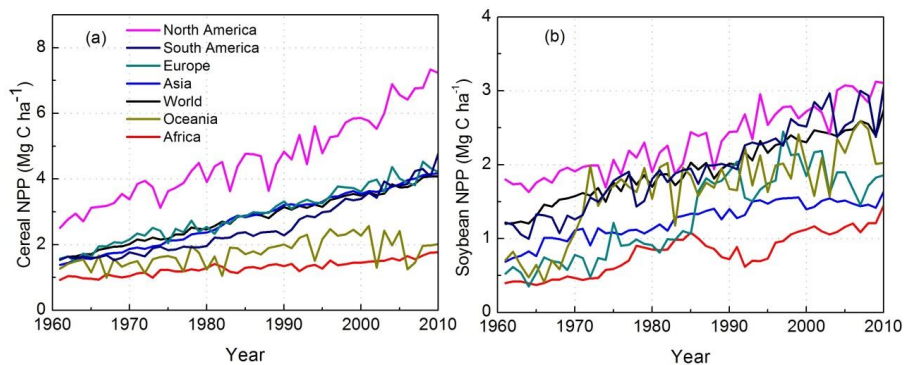


713  
 714  
 715  
 716  
 717

Figure 7: Country-based comparison of simulated and observed cropland productions (Tg) before (a) and after (b) calibration. Each country consists of five dots representing the five decadal mean values, respectively.



718  
719 Figure 8: Mean cropland NPP from 1997 to 2003. VEGAS modelled patterns (in units  
720 of Tg C per 0.5° grid cell, upper panel) show major productions in the agricultural  
721 areas of North America, Europe and Asia (the lower panel shows the mean crop NPP  
722 based on the FAO statistical data from Navin Ramankutty (<http://www.earthstat.org/>)).  
723  
724



725

726 Figure 9: Cereal and soybean NPP at continental scales over the last 60 years derived  
727 from FAO yield data. Note that the scales are different.

728

729